PAPER • OPEN ACCESS

Investigation on the multiple plies structure of aluminum-lithium alloy and glass fiber composite with respect to deformation failure

To cite this article: Syed Qutaba *et al* 2023 *Mater. Res. Express* **10** 016507

View the article online for updates and enhancements.

Materials Research Express

PAPER

Investigation on the multiple plies structure of aluminum-lithium alloy and glass fiber composite with respect to deformation failure

Syed Qutaba[1,2,*] ⬤, Mebrahitom Asmelash[1] and Azmir Azhari[1]

[1] Faculty of Manufacturing and Mechatronic Engineering Technology, Universiti Malaysia Pahang, 26600 Pekan, Pahang, Malaysia
[2] Department of Textile Engineering, BUITEMS, 83000 Quetta, Pakistan
[*] Author to whom any correspondence should be addressed.

E-mail: engrsyedqutaba@gmail.com

Abstract

The deformation behavior and mechanical properties based on the aluminum-lithium alloys (FMLs) was investigated to optimize the manufacturing process and further interface interaction. The primary structures of the FML composites were made with two sets of plies. From there, six secondary composites with different fibre sheet orientations were made. Then, interlaminar tensile, flexural, and peeling properties of FMLs were tested. The fiber orientation role in the case of failure behaviors of FMLs under different conditions was also revealed. The results have indicated that the plies design significantly enhanced the interlaminar properties of the FMLs and orientation of fiber laying has significantly affected the flexural strength. The peeling test has shown higher fiber-to-metal interfacial bonding with the value of $\geqslant 80\,\mathrm{N\,m}^{-2}$ over metal-to-metal adhesion. The plies increase the mechanical properties of composite based at fiber orientation and thickness, but too much impairs performance. The 3/2 plies showed a value of $\leqslant 385$ MPa, which has better results in axial structure analysis than over 4/2 composite layers. The peak values appeared under different parameters like adhesive bonding and parallel fiber orientation, represented in the qualitative analysis section. The surface microscopy of aluminum-lithium alloy sheet and cross-section failure morphology of composite has been done at a different sighting. Surface characterization, fiber orientation breakdown, and deformation morphology have been studied concerning alloys' elongated grains and micro pits.

1. Introduction

Fiber Metal Laminates (FMLs) are hybrid materials that combine remarkable deformation resistance and high strength of fiber reinforced composite plies, where metal layers and fiber-reinforced composite (FRP) plies are alternately placed [1, 2]. According to the second generation of FMLs, GLARE (Glass Laminate Aluminum Reinforced Epoxy) is well-known for its widespread use on A380 fuselages, where it processes high strengths, good fatigue resistance, and impact resistance [3, 4]. Fiber metal laminates are now high-performance materials widely used in aviation, resulting in their widespread use in fuselages and wings of big aircraft [5]. The Airbus A380 was able to save 794 kg of weight by using Glare in the top fuselage skin [6].

Many researchers [7, 8] have produced higher-performing FMLs, such as CARE (aluminum with carbon fibers) and TiGr (titanium with carbon fibers). As a result, CARE experiences severe galvanic corrosion, whereas TiGr is the most valuable and also has the shortest hardenability. With respect going to limit its commercial practical application aluminum-lithium alloys have greatly increased in recent years due to their better density, strength, and stiffness. The All-Russia Research Institute of Aviation Materials (VIAM) concentrated on researchers who compared aluminum-lithium 1441 alloys to GLARE, but the results ended up falling short of their expectations.

Surface treatment processes help enhance the properties of the material. Qutaba *et al* have described the surface treatment process in four categories which are mechanical, chemical, electrochemical, and case hardening. In the mechanical surface treatment process, hot and cold have imparted. In hot treatment, mostly

annealing, rolling, and welding is the most frequently used process in the mechanical industry with the help of heat. In cold treatment, critical processes are cold rolling and peening inducted into some mechanical parts without heat. The electrochemical process was introduced with cathode and chemical reactions treatment at the material surface [9, 10]. An electrochemical reaction is any process caused or accompanied by the passage of an electric and typically includes the transfer of electrons between two solid and liquid substances [11]. In critical rolling and solution-aging treatments are the most important operations once producing the metal layers of FMLs. The aging and shaping process outcomes are stronger and have a greater elastic modulus [12, 13].

In the fabrication of composite matrix, GLARE and FMLs, it is necessary to have three substrates like metal, fiber, and liquid adhesive [14]. A spray to the adhesive layers or at least a priming layer on the metal surface lead to interfacial bonding [15, 16]. It has been revealed that it diminishes contact angle, tends to increase fiber surface area, and strengthens surface roughness. The bonding strength of the adhesive layers has undoubtedly improved the interlaminar properties, strength, and deformation of the FMLs. An excessive amount of adhesive, on the other hand, reduces the volume fraction of glass fibers in the overall laminate, compromising the mechanical properties of FMLs [17, 18]. Additionally, the effect of fiber volume fraction (%) and composites with volumetric amounts of fiber are assessed [19].

To assess the material's strength, the composite's tensile properties were utilized, and modal testing was performed to determine the composite's dynamic qualities [20]. Due to the adhesion of bonding and mass volume fraction, the axial dimension strength of the solo material and the matrix are only marginally different from one another [21]. When it helps to prepare the metal layers for the composite and strengthening process, the most important processes are the cold rolling and ageing treatments [22]. By heating the alloy 299 to 410 °C, the annealing process resets the crystal structure and makes a new batch of slip planes that have yet to be used [23].

A significant amount of research has been done on the aging and forming processes of the novel alloy used as the metal layers of FMLs. The treated aluminum-lithium alloy has higher strength and elastic modulus than the 2024 alloy, according to the findings. The novel alloy's advantageous properties will also result in an improvement in the performance of FMLs [24, 25]. The decent wettability of epoxy is widely regarded as advantageous to the adhesion of fiber-epoxy composite laminas and aluminum alloy sheets. The wettability of a liquid is normally determined by measuring the contact angle of the liquid on the surface of an aluminum alloy sheet. On the other hand, the contact angle of epoxy is difficult to measure due to its high viscosity and poor mobility [26–28]. The addition of lithium into aluminum improve modulus and decrease density even before compared to conventional aluminum alloys, lithium-containing aluminum alloys 8090 are of significant current interest in the aerospace and aircraft industries [29, 30]. Few commercial aluminum-lithium alloys before 8090 have emerged for use in the aerospace industry [31].

The other fact, the epoxy is difficult to infiltrate into the porous structure on the aluminium alloy sheet without pressure; thus, FMLs based on aluminum-lithium alloy were prepared in this study. The alternatives have included fiber replacement and metal layer replacement. Novel aluminum alloys, particularly aluminum-lithium alloys, have shown to be more damage resistant than traditional 2xxx and 7xxx series aluminum alloys in recent years [32–36]. Aluminum-lithium alloy has a wide range of applications in the aerospace industry due to its appealing properties, which include lower density, increased strength, and improved stiffness [37–39].

In this research study, embedded a systematic research on development of two different set of composite plies 3/2 (A/G/A/G/A) and 4/2 (A/G/A/A/G/A) (See figure 1) has development under the three types of different fiber orientation which based on layering angle, describe in the figure 2 and table 2. The evaluation of floating peeling, tensile, bending properties has been performed to reaches the prime objective of structure failure behavior, to confirm explicitly inferred experimentally and verify the reinforcement effect of aluminum-lithium alloy. The basis of the density and role of thickness in the composite technology which effect mechanical properties of FMLs. Further, some new facts about interfacing bonding between (fibers to metal) & (metal to metal) zone had noted during peeling tests. The scanning electron microscopy (SEM) and surface morphology has observed. It would be expecting that this work will provide a new way for the improvement of mechanical and damage initiation of the fiber metal laminate (FMLs).

2. Experiments

2.1. The preparation of FMLs

In recent years, the aluminum-lithium alloy 8090 has been associated with the large commercial aircraft manufacturing industry. It belonged to the Al–Cu–Li family, with a Cu/Li ratio of 5.29. The nominal chemical composition of the aluminum-lithium sheets (2 mm thick, T8 state) used in this study is shown in table 1. During the manufacturing process, the 0.5 mm aluminum-lithium layers shown in figure 3 were first prepared. Additionally, the aluminum-lithium layers were surface treated to enhanced the strength to improve bonding
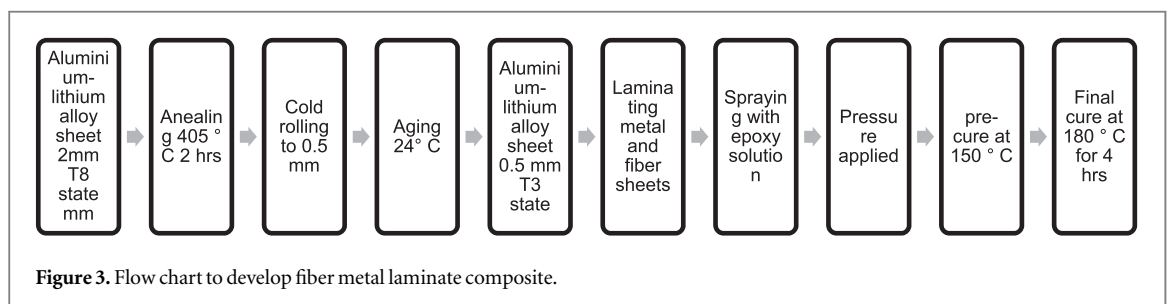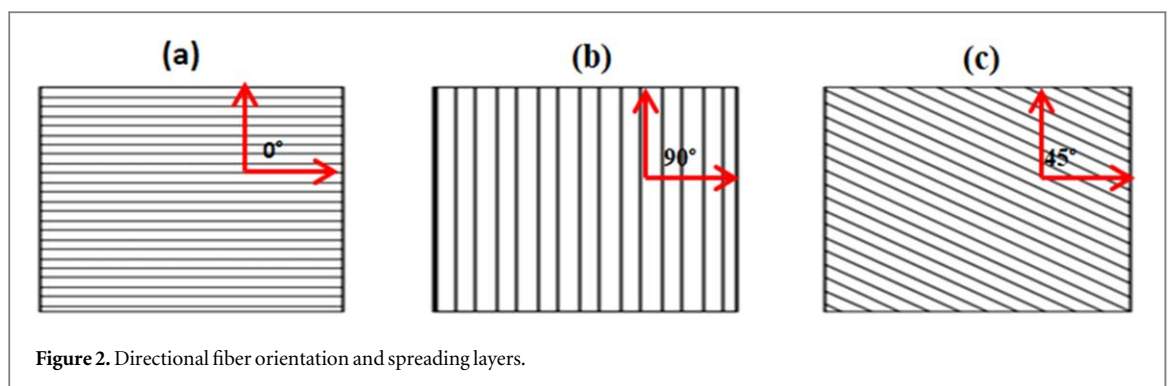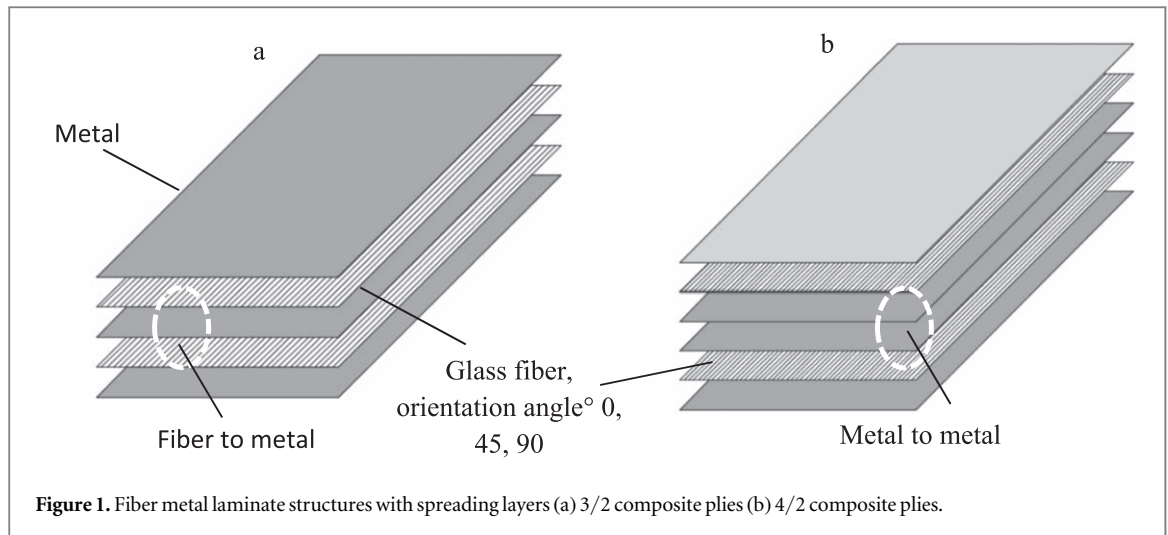
Figure 1. Fiber metal laminate structures with spreading layers (a) 3/2 composite plies (b) 4/2 composite plies.

Figure 2. Directional fiber orientation and spreading layers.

Figure 3. Flow chart to develop fiber metal laminate composite.

Table 1. Chemical composition of raw aluminum-lithium alloy sheet 8090.

Al-Li	Cu	Mg	Ag	Zr	Mn	Zn	Al
2.2–2.7	1.6	1.3	0.34	0.11	0.29	0.32	Rest

with fiber-reinforced composites [40]. After being heated to a high temperature during annealing, metal is passed through rollers at temperatures below its recrystallization and thickness. This is called cold rolling [41]. In the next step of the treatment process, aging is used to make the metal stronger by causing the alloying material to form a precipitate inside the metal structure [42]. It was decided to construct a rough surface with chemical treatment for 5 min in the chamber. The used of a heated chamber and chemical treatment has to develop the rough surface which as shown in microscopy figure 6. After the anodizing process on the metal layers, the aluminum-lithium layers were sprayed with a quantity of 35 g m^{-2} adhesive, while the top and bottom layers in the FMLs were not in touch with any liquid.

Sinopec petrochemical developed the JHY 601 structural adhesive, which is a high-temperature resistant and two-component (resin + hardener) epoxy system. The manual spray cycle system was used to control the spread quantity, which had been confirmed by weighing. The mass volume fraction related to fiber and epoxy was 0.10.
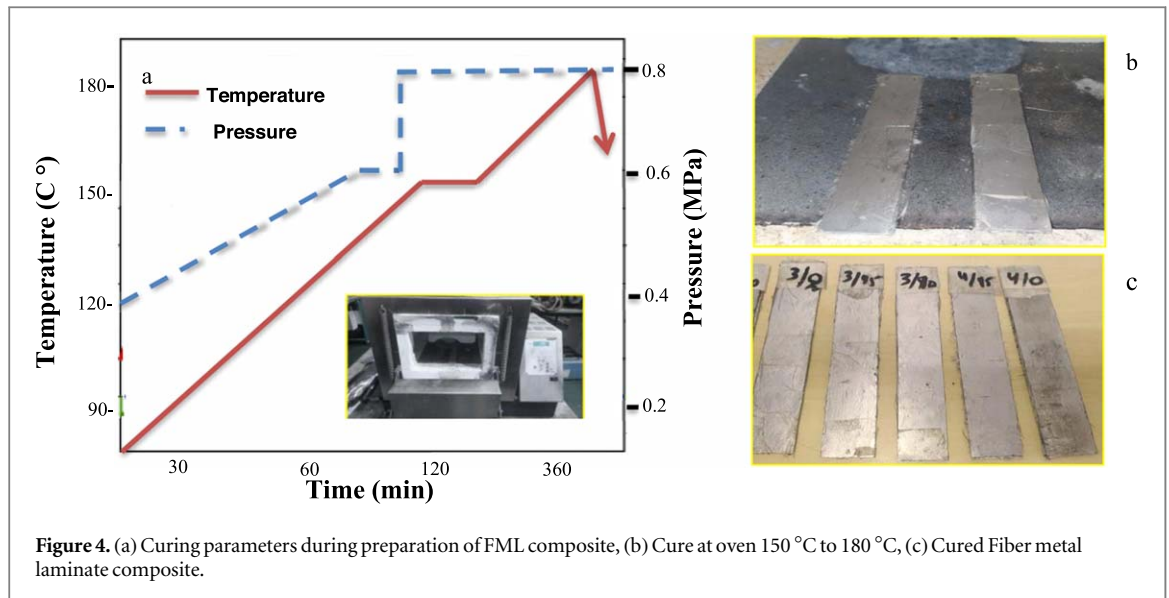
Figure 4. (a) Curing parameters during preparation of FML composite, (b) Cure at oven 150 °C to 180 °C, (c) Cured Fiber metal laminate composite.

Typically, the adhesive has to be injected into the metal layers within 12 h following anodizing in order to effectively protect the surface's roughness. The 3/2 and 4/2 FMLs are consisting of three and four aluminum-lithium sheets and two glass/epoxy plies were manufactured as the two distinct plies combinations.

The laminates were reinforced with the pre-treated; strengthen aluminum-lithium 8090 layers and S4-glass/epoxy prepregs with a thickness of 0.125 mm. During the spreading of layers' process, the metal layers and prepregs were adhered to the laminating design shown in figure 1. The six different fiber prepregs angles (°) were used during the fabrication. These angles are classified into three categories shown in figure 2. These orientations have been prepared by a perpendicular directional glass fiber sheet.

The GSM (Gram square meter) of the glass fiber sheet was around 300 and the ends per inch were 24. The Fiber layers and aluminum-lithium 8090 sheets have been laminated with mentioned plied and fiber angles. After the laying of sheets, the solution of epoxy is applied in between layers and pressed with hydraulic pressure around 0.68 MPa. The pressed sprayed pieces of the composite are tenant-up in a furnace for curing at an initial temperature of 150 °C shown in figures 3 and 4(a). After 2 h the pressure at the pre-cure surface of the composite piece was around 0.88 MPa, for low viscosity of epoxy resin besides increasing the temperature slightly to fix the epoxy solution until more than 4 h. The two component-based adhesive systems have always needed pre-cure temperature to remove the air and less viscosity for better implementation.

Finally, 3/2 and 4/2 FMLs (figure 4(b)), the most common design for Glare and other FMLs was created using aluminum-lithium alloy 8090 sheets and glass/epoxy plies.

2.2. The testing of FMLs

The density of FMLs was determined using the ASTM D792 water displacement method. The tests were carried out using 10 mm×10 mm specimens in a standard atmosphere of 23 ± 2 °C and $50 \pm 5\%$ relative humidity. The ASTM D3039 standard was used to investigate the tensile properties of FMLs with a displacement rate of 1 mm min^{-1}; a universal testing machine (UTM) model (INSTRA 3369) with a capacity of 50 KN was used to investigate the values. Meanwhile, a flexural test was carried out using the three-point bending method. The specimens were 75 mm×10 mm in size, with a loading rate of 1 mm min^{-1}. Furthermore, the ISO 14125 Large-deflection corrections were used to calculate the flexural strength. For the interlinear properties, the floating roller peeling tests were selected in this study. Meanwhile, using a loading rate of 50 mm min^{-1} and a floating roller peeling test based on ISO 4578, the average peeling load between metal layers and pre-pregs was determined.

2.3. Surface characterization and morphology

A Scanning electron microscope is the most common tool for determining the microstructure of aluminum alloys and is recommended for use before electron optics, which has a size range of 0.1 μm. It's useful up to magnifications of about 1500 X, where even the tiniest grains or particle can be seen. Laser microscopy has identified the second-phase structure and layers of sufficient size as compared to another electrons microscopy. Microscopic sample had been prepared through wire electric discharge cutting machine, due to the accuracy and to avoid burnish at the composite edges.
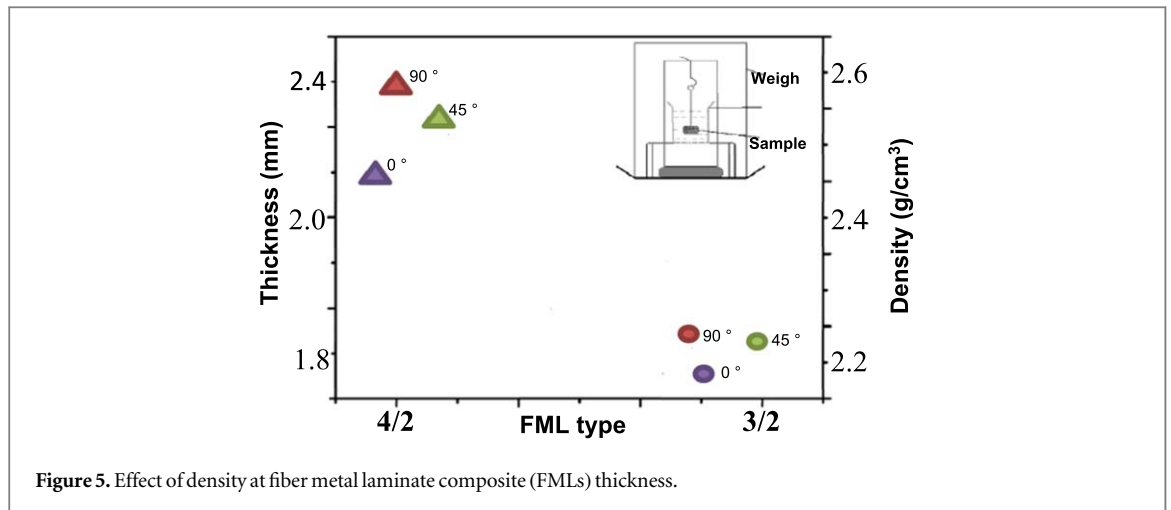
Figure 5. Effect of density at fiber metal laminate composite (FMLs) thickness.

The surface morphology of a pre-treated aluminium alloy sheet is depicted in figures 6(a), (b). Due to the effect of micro grains and convicted through an annealing process, some uneven and even pits are visible on the sheet surface. The pits can improve the adhesion strength by increasing the bonding area, figures 6(c), (d) shows that after annealing and cold rolling treatment, some different visions of the treated sheet have elongated grain structures observed in characterization. A dense oxide film is formed on the aluminum alloy sheet surface during the electrochemical reaction of annealing and aging process. The strengthening process has produces the transformation of predominantly layers and continuous grain boundaries. When an alumina barrier layer forms on the surface of the aluminum alloy sheet, several stages of porous oxide growth occurs. These films are most likely anodic due to aluminum alloy can form compact after the electrochemical reaction. These Anodic aluminum oxide (AAO) film with a thickness ranging from 20 to 100 μm [43]. Figure 6(e) describes the characteristics of the dense oxide film measured through an optical laser microscope.

Figures 7(a), (b) is a cross-sectional depiction of composite plies. Cross-sectional views describe the primary structure of both types of layering plies. Figure 7(a) clearly describes the uniformity in the structure and the metal layers are slightly porous and dense. While figure 7(b) shows porous and dense metal layers with some weak metal-fiber adhesion.

3. Results and discussion

The following characteristics of Fiber metal laminate performance are being identified, emphasizing the main comparison between the two structures of composite employed in the study, each with a distinct fiber orientation. The entire below test has been performed according to the physical aspect of composite technology.

3.1. Effect of density on fiber metal laminate

The increasing and decreasing of sheet quantity in the composite naturally affects the results in the thickening and density of FMLs, as shown in figure 5. However, the thickness has also led to the density of FMLs because the adhesive layers have a lower density (1.21 g cm^{-3}) than pre-pregs and aluminum-lithium layers. The thickness of the composite has affects the density related with strength and physical properties of the material. Figure 5 represented that 3/2 structure hasn't much effect on the density, and also the fiber orientation is not being considered a factor to increase density. The density of 4/2 structure has an effect slightly higher as compared to 3/2. The reason behind is that two metal layers are interlacing each other so; it could gain a more adhesive solution as compared to fiber and metal structure. Another concern, which has been highlighted in figure 5 related to fiber orientation (°). After testing the dimensions, it has been noticed the number of fibers between the composite affects the thickness. As 90° has contained more fiber as compared to the other two fiber orientations, it has been noticed the number of fibers between the composite affects the thickness and density. The composite hand lay-up method has random errors during development stages, so to recover the errors it has recommended to make more samples and tests. In actual, each sample was prepared 5 times and the error difference was found to be less than 5% on basis of density. Furthermore, out of 5 prepared samples for each case only 3 samples were used for further testing.
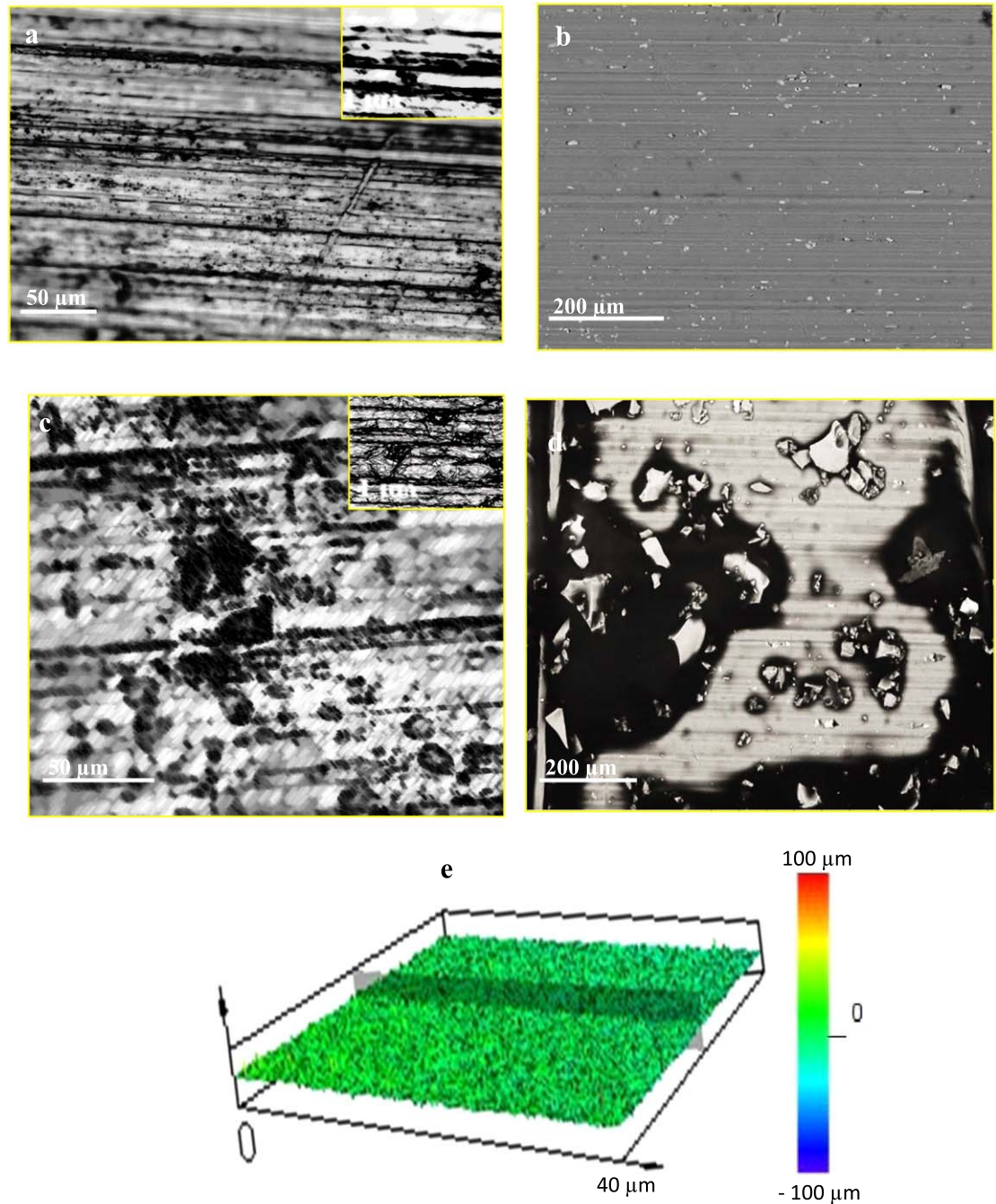
Figure 6. Surface microscopy and morphology of Al-li alloy, (a), (b) Pre-treated, (c), (d) after treated with annealing, (e) Topography of dense oxide film.

3.2. Analysis the physical properties of fiber metal laminate

In the case of composite, physical properties play an important role in the development and future of composite life. The interlaminar properties of hybrid materials are crucial, as they impact the overall performance of FMLs. In this paper different physical tests have been performed on the material for a better understanding of reinforcement as reacted by fiber metal laminate.

3.2.1. Tensile strength

The tensile strength has been shown in different aspects of six types of composite plies structures. The main two types have analysis for better future formation. Undoubtedly, the spreading layers have a substantial impact on the interlaminar characteristics of FMLs.

The adhesive layers are very beneficial to the tensile resistance of the FMLs, as shown in figure 8(b). However, the fiber layers and adhesive with the aluminum-lithium layers were completely resistant to the axial forces at
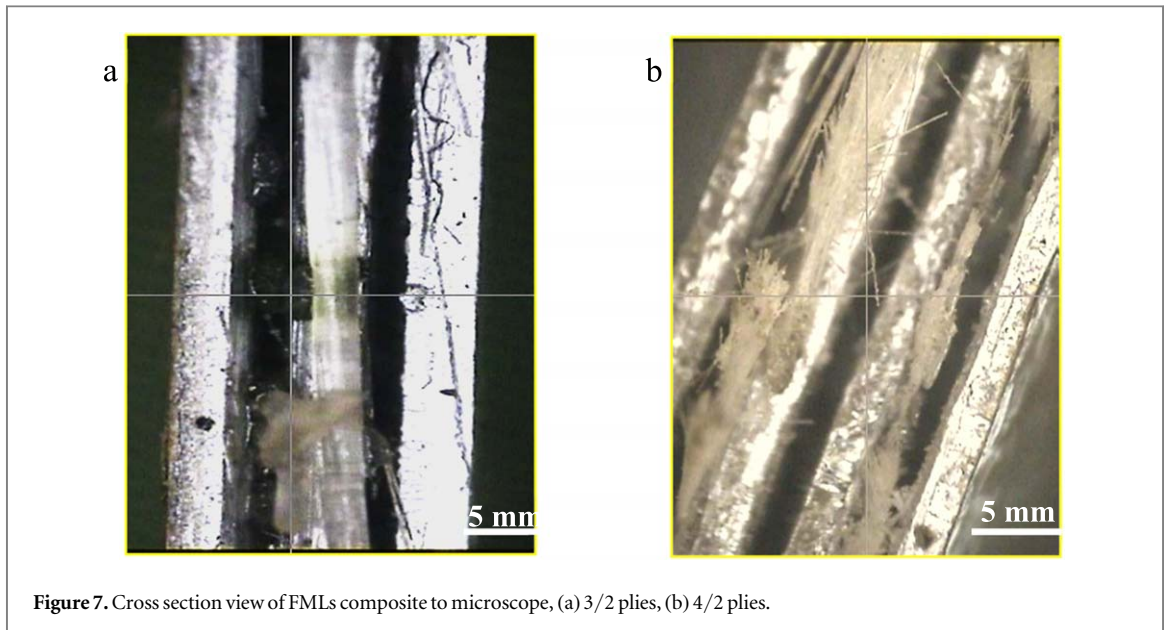
Figure 7. Cross section view of FMLs composite to microscope, (a) 3/2 plies, (b) 4/2 plies.
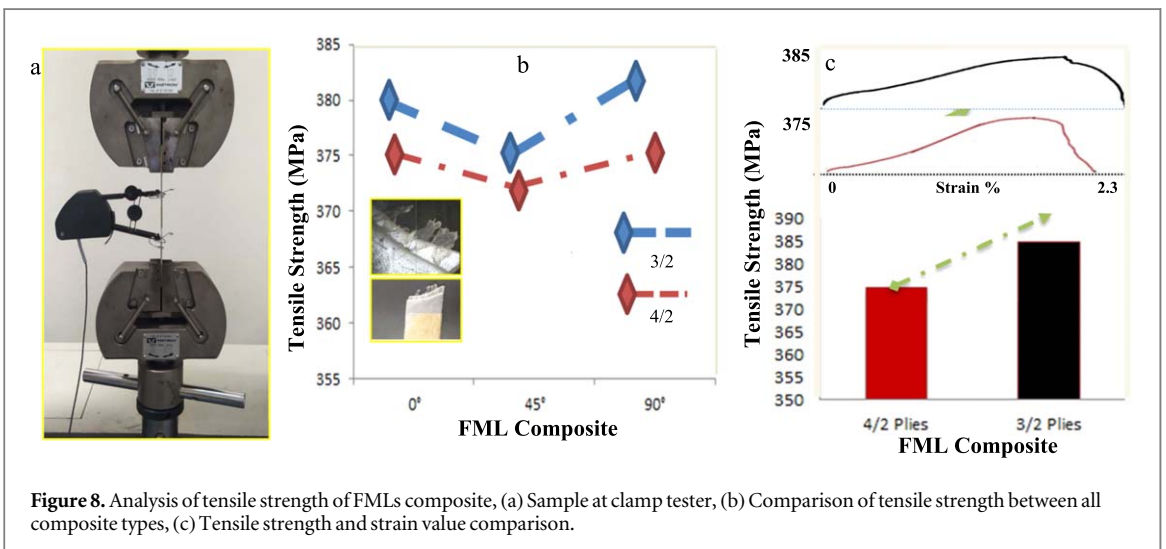

Figure 8. Analysis of tensile strength of FMLs composite, (a) Sample at clamp tester, (b) Comparison of tensile strength between all composite types, (c) Tensile strength and strain value comparison.

composite. With the increasing fiber orientation angle, the strength of the metal/prepregs interfaces causes delamination and damage to the prepregs. Figure 8(b) shows that the tensile strength of both composite plies 3/2 & 4/2 is nearly identical to each other, though the interfaces of metal/prepregs are usually weaker than those of fiber/epoxy. It has been revealed after tensile tests the 3/2 composite reaches the average value of 385 MPa, and another side identical composite which has one more layer as the previous one showed the average value of 375 MPa.

The fiber orientation has revealed some variation in a tensile result like 0° orientations as it reaches the 385 MPa, cogitates orientation 45° shows the value of 378 MPa and last orientation 90° reaches the value of 379 MPa. As other 4/2 composite plies have reach the average value of 375 MPa, but ⩽than 3/2 composite tensile value even high in thickness and density. The fiber orientation has revealed some variation in tensile results as case of 4/2 plies, like 0° orientations as it reaches the 375 MPa, cogitates orientation 45° shows the value of 367 MPa and last orientation 90° reaches the value of 379 MPa. Figure 8(b) has also revealed the breakage of the fiber after the tensile strength and showed the angular image of the composite tear. The strain rate has been shown by the behavior of FML composite as around 2.3% in figure 8(c).

The most dominating strain belongs to 3/2 plies, and 4/2 plies haven't sufficient less than ⩽2.3. Figure 8(c) has revealed the failure of higher density and thickness composite at against of axial strength. Figure 9 has shown the fiber layer behavior and breakage during the axial tensile loading and Scanning electron microscopy of the damage fiber layers. The fiber orientation of 0° is placed along the axial direction of the samples during the tensile test as shown in figure 9(a). Whereas, fiber orientation of 90° was placed perpendicular to axial direction of the sample during tensile test as shown in figure 9(a). Figure 9(b) shows a microscopic view of the 0°
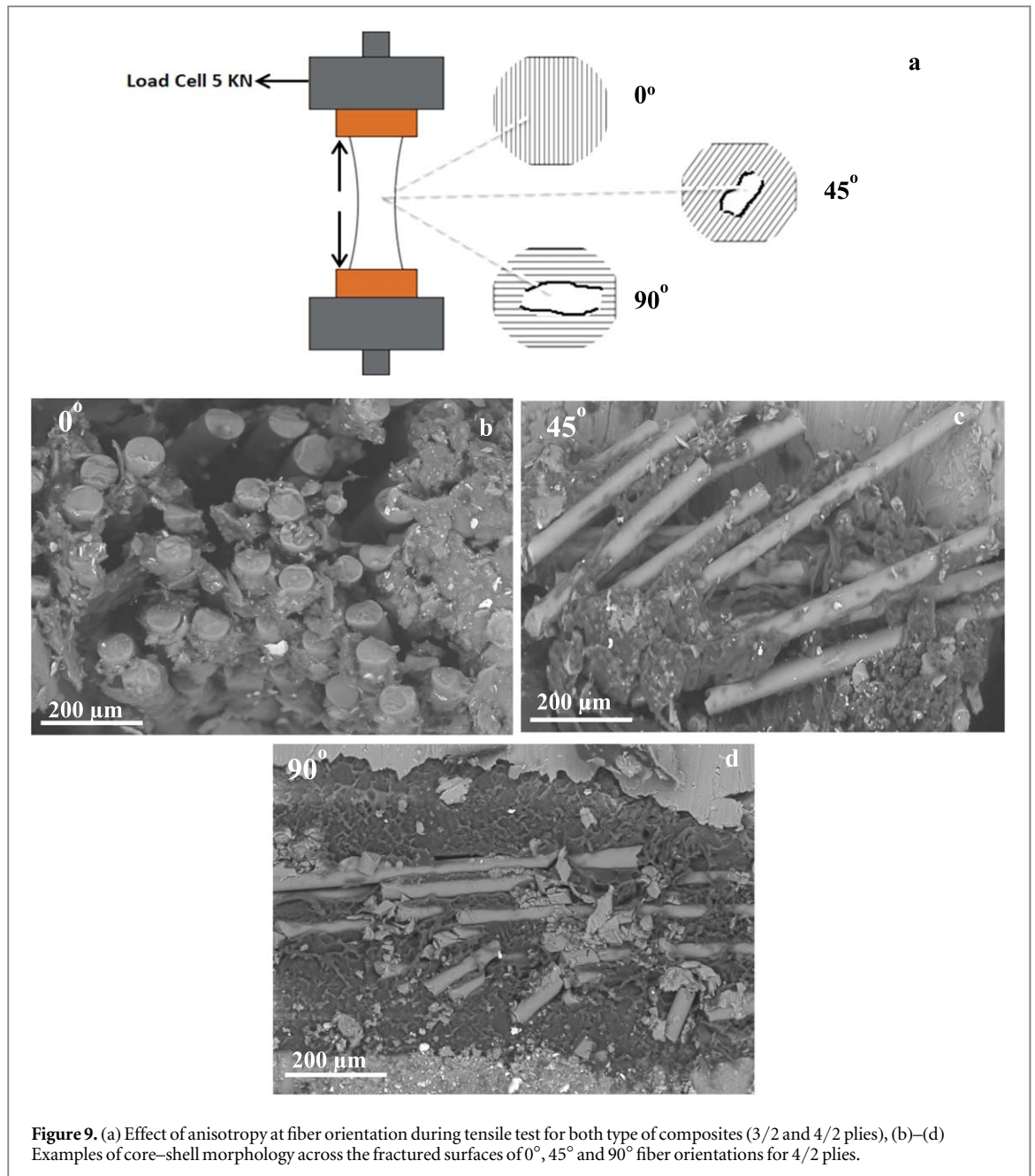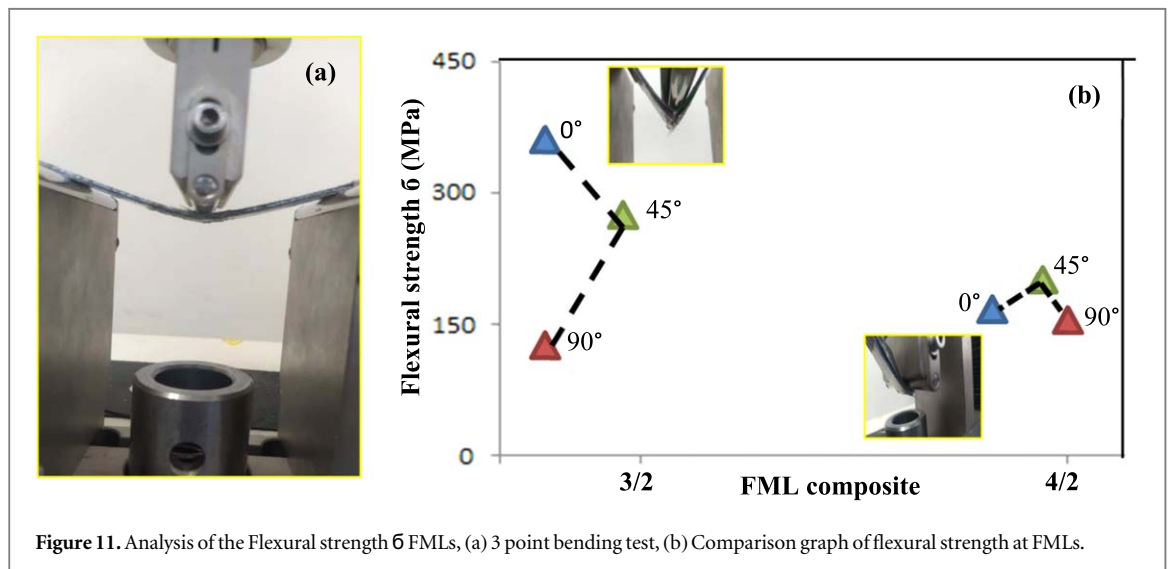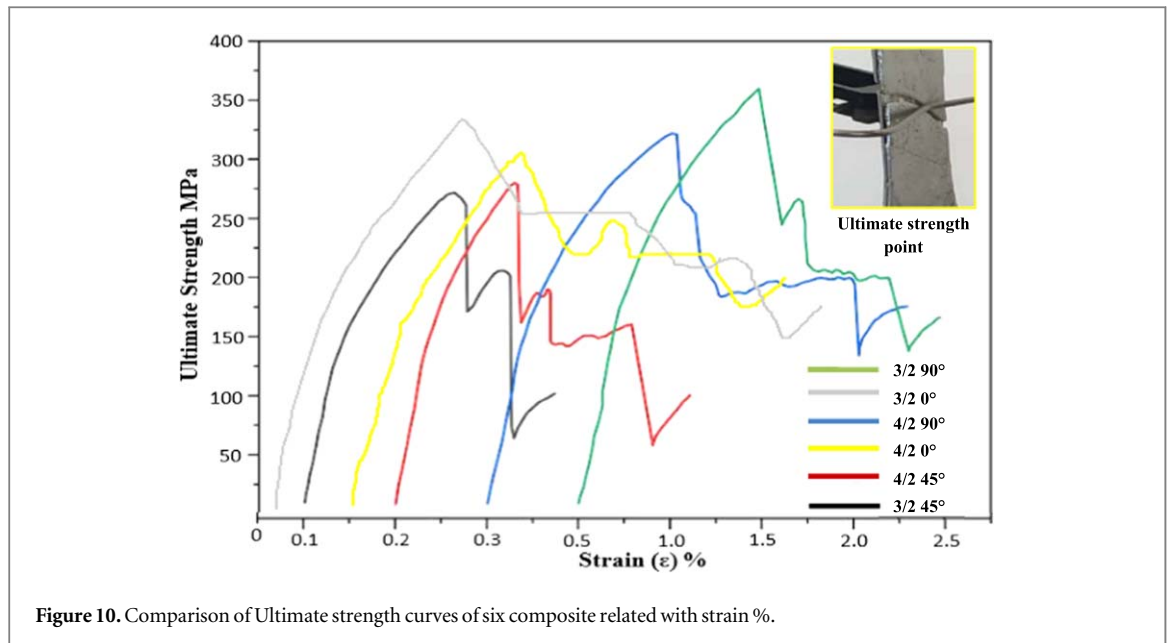
Figure 9. (a) Effect of anisotropy at fiber orientation during tensile test for both type of composites (3/2 and 4/2 plies), (b)–(d) Examples of core–shell morphology across the fractured surfaces of 0°, 45° and 90° fiber orientations for 4/2 plies.

orientation, which resisted the force similar to metal sheets. However, fiber layers were not behaving with additional resistance, so the force value is less than 90° orientations due to similar fiber breakage. The maximum strain % in these orientations corresponds to fracture strain. The effect of mold flow direction on stress–strain response is significant at 0° with strain rates. In case of 45° fiber orientation figure 9(c) SEM has represent that more load as compare other two fibers angle, so sheet had resist the force and faced dismantling the fibers. Figure 9(d) SEM analysis has noted behavior of 90° fiber layers breaking. The fiber sheet had bear load with help of epoxy resin, so the breakage had very uneven.

The mass volume of fiber (%) has affect during load due to epoxy resin and stretching strain, while steaking with weak bonded area of the FMLs composite. The facts have relation between fiber volume fraction % and fiber orientation (°). These dual factors are very dominant in the composite tensile analysis [20]. The fiber volume fraction and mass volume fraction of material affect the tensile properties of the composite, equality in fiber volume fraction is more effective [44]. Figure 10 has shown the comparative performance of all six types of composite with respect to the ultimate strength and total strain % during the axial loading test.

3.2.2. Flexural strength б
The effect of the flexural strength has been shown in different aspects of six types of composite structures. The main two types have analysis for better future formation. Undoubtedly, the properties of FMLs are significantly

Figure 10. Comparison of Ultimate strength curves of six composite related with strain %.

Figure 11. Analysis of the Flexural strength б FMLs, (a) 3 point bending test, (b) Comparison graph of flexural strength at FMLs.

affected by the spreading layers, thickness, and density of the composite. Even more impressive is the influence that the adhesive has on the flexural characteristics of the material. The quantity of flexural strength that was investigated steadily higher as it approaches the high value (refer to figure 11(b)). Similar to the tensile strength has affected the influence of adhesive.

Figure 11(b) has revealed that the maximum value of flexural strength (б) become around 385 MPa, with the fiber orientation 0°, beside the combination of 3/2 plies composite. The identical plies have also revealed the different values of flexural strength (б) at the different fiber orientation angles. Like 45° is around 270 MPa and angle has a lift to more the value becomes 147 MPa. The 4/2 plies composite has shown a very low value of flexural strength (б) in figure 11(b). The 0° fiber orientation in the 4/2 has provided the value of 154 MPa, as follows 45° fiber orientation was showing identical around 158 MPa. The last combination of fiber orientation is 90° which has followed the trend of the previous orientation and the value is 152 MPa. Figure 11(b) reveals that the 3/2 plies composite has more flexural resistance force as compared to the increasable sheet combination of 4/2 plies.

The flexural strength is also affected by two conflicting variables, namely the thickness of the laminate and the improvement of interfacial adhesion. Figure 12 has revealed some numerical values related to strain and strength of two different combinations of composite. The graphs line of six different samples is displayed, providing the information related to flexural strain (ε) %. Figure 12(a) has shown that in 3/2 plies some fiber orientation like 0° and 45°, reached towards with better flexural resistance. These composite plies have
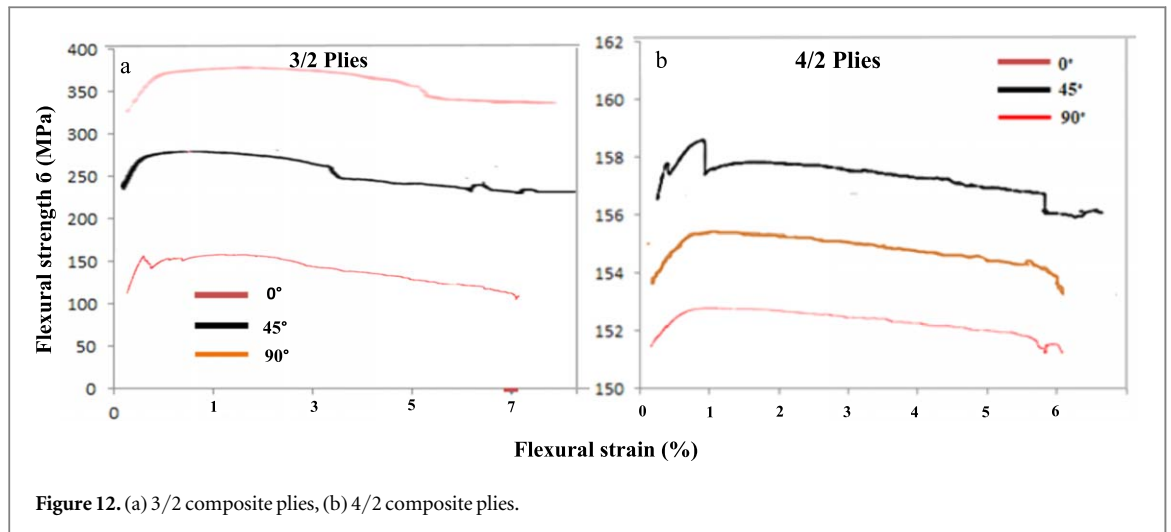
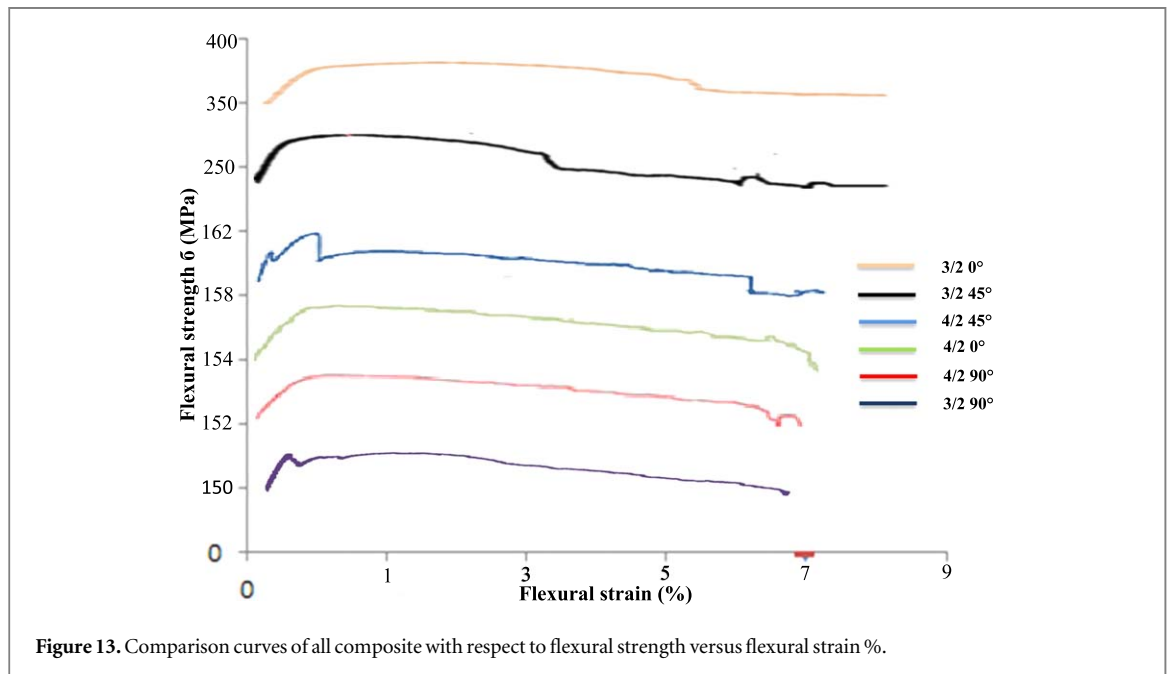**Figure 12.** (a) 3/2 composite plies, (b) 4/2 composite plies.

Figure 13. Comparison curves of all composite with respect to flexural strength versus flexural strain %.

interfacial bonding with fiber and metal, so they provided the maximum strain of 7%. The last fiber orientation composite has shown a value of strain ⩽7%.

Figure 12(b) has revealed few numerical values connected with strain and strength of different fiber orientation combinations of composite plies. The graph's line of 3 different samples is displayed, providing the information concerned with flexural strain %, revealing that in 4/2 plies composite all-fiber orientation reached with maximum flexural strain % is around ⩽6. These composite plies have interfacial bonding with metal and metal, so they provided a maximum strain of 6%.

Mostly 3/2 plies have better value as compared to 4/2 composite due to high bearing load capacity. Furthermore, comparing the fiber orientation (°) in the highlight of figure 11 has revealed that 0° and 45° take part in influencing the resistance of bending strength. These composite plies have interfacial bonding with metal and metal, so they provided a maximum strain of 6%. Figure 13 has graphically presents the performance index of all the composite and bending behavior. The flexural stress has variate at every composite type, but strain of value nearly to each other and very rare variation can be seen in figure 13.

The deformation behavior has depended upon the directional fiber layers which resist the bending load. In the case of fibers, the angle of 0° has absorbed more force as compared to other angles shown in figure 14. The sheet of fiber and epoxy are well resistant and more bent when the load is applied represent in figure14. The fact has been noted that long-length fiber from width to width is quite affected by resistance forces. However, the other two angles 45° and 90° have different behavior as compared to the 0° orientation. Composite has
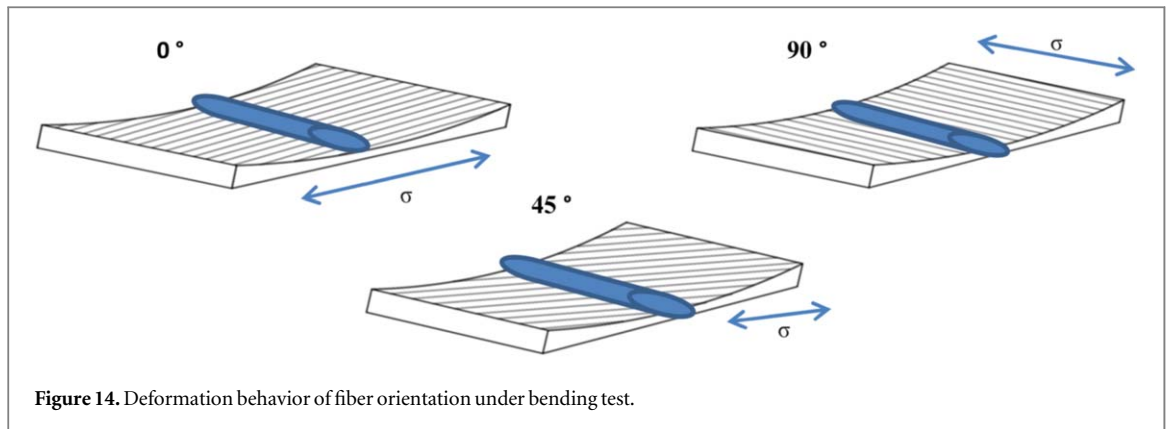
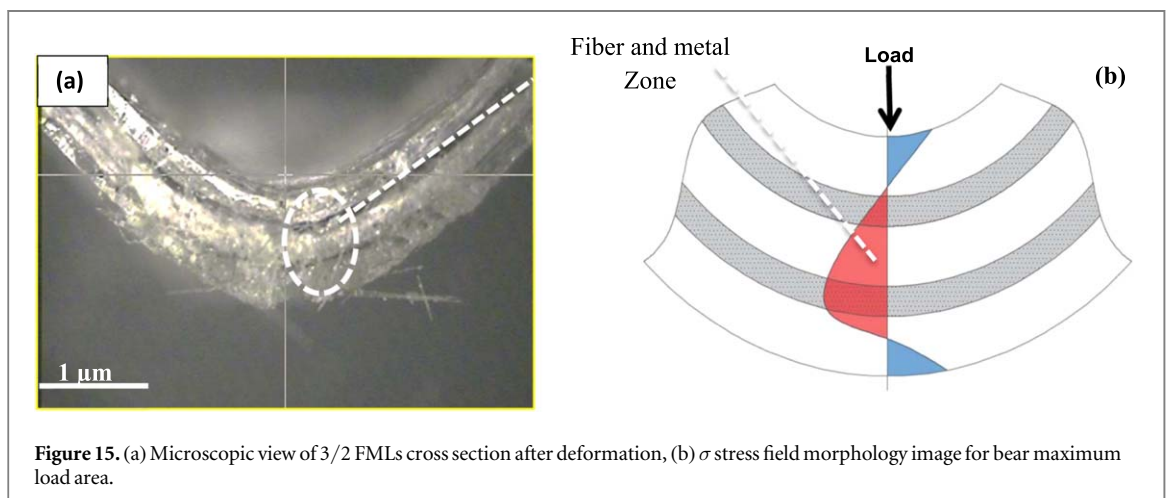**Figure 14.** Deformation behavior of fiber orientation under bending test.

Figure 15. (a) Microscopic view of 3/2 FMLs cross section after deformation, (b) σ stress field morphology image for bear maximum load area.
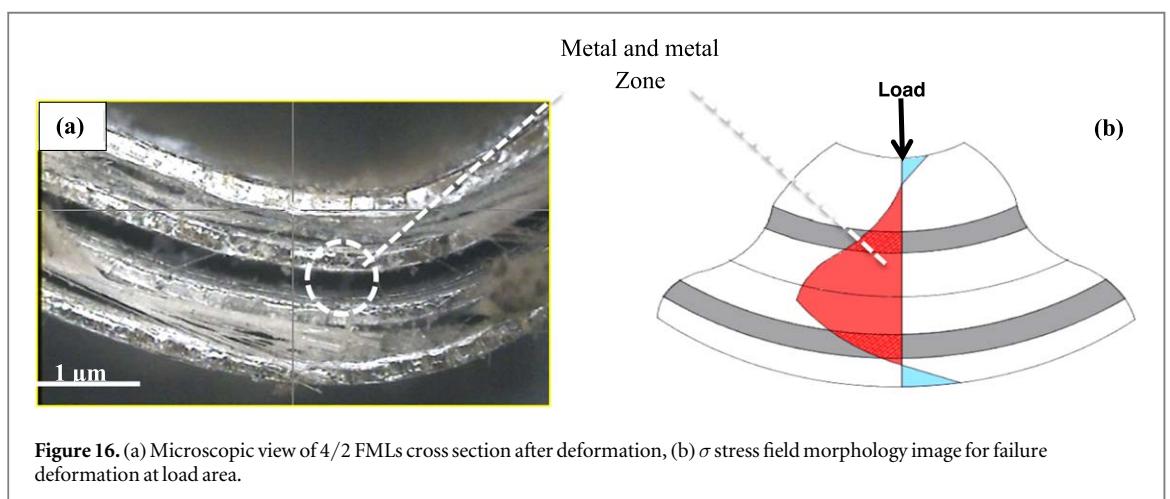

Figure 16. (a) Microscopic view of 4/2 FMLs cross section after deformation, (b) σ stress field morphology image for failure deformation at load area.

manufactured from 45° and 90° show less value of Flexural strength and strain as compared to 0° orientations. It has been analyzed that fiber length affects the bending stress of the composite.

During the bending and deformation of 3/2 plies composite, the interfacial bonding hasn't shown any gap during deformations. Even no breakage has been noted during the optical microscopy as shown in figure 15(a). Figure 15(b) has revealed the morphology of the tension zone by σ stress distribution field during the flexural strength of 3/2 composite plies[45]. The blue morphology zone has shown some minor crankiness at the top and bottom layer of the composite in stress distribution [46]. The same figure has revealed the behavior of fiber and metal bonding during the delamination, present in the red color morphology. The red zone has shown that more resistance of flexural strength needs to bear the top fiber and metal layer and it observed the force instead to reduce the impact on the lower layers of fibers.

Figure 16(a), it has reveal that during the bending and deformation of 4/2 plies composite, the interfacial bonding has displayed distance gap during deformations in the structure of composite. Even separation has
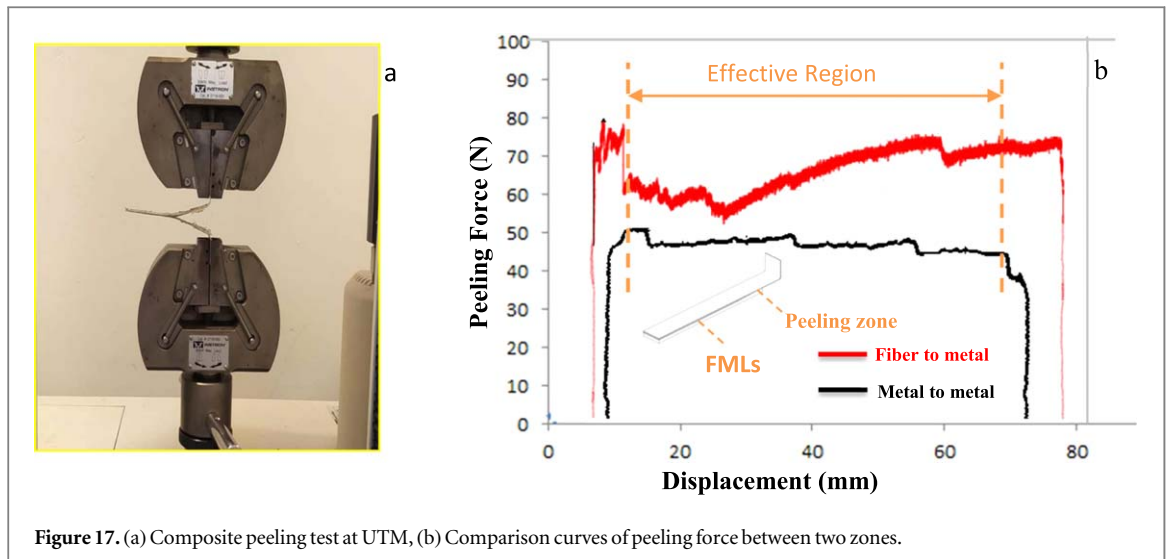
Figure 17. (a) Composite peeling test at UTM, (b) Comparison curves of peeling force between two zones.

Table 2. Classification of composite with sheet angles.

Classification	Angle°	Design
3 Aluminum- lithium alloy sheet with 2 sheets of directional glass fibers	0°	
	45°	
	90°	
4 Aluminum- lithium alloy sheet with 2 sheets of directional glass fibers	0°	
	45°	
	90°	

noted during the optical microscopy between the layers. The σ stress field distribution has noted failure during the metal to metal bonding with adhesive. Figure 16(b) has briefly detailed the morphology of the tension zone during the flexural strength of 4/2 composite plies. The blue morphology zone has shown some minor crankiness at top and bottom layer of composite in through σ stress morphology. The failure imaginary reason has revealed between metal and metal bonding during the delamination, present in the red color morphology. The red zone has shown that less resistant of flexural strength to inhaul the top metal and lower metal layer and couldn't observed the force with instead to reduce impact on the lower layers of fibers. The microscopy has already revealed that composite was separated in two parts when the load has imparted and increased.
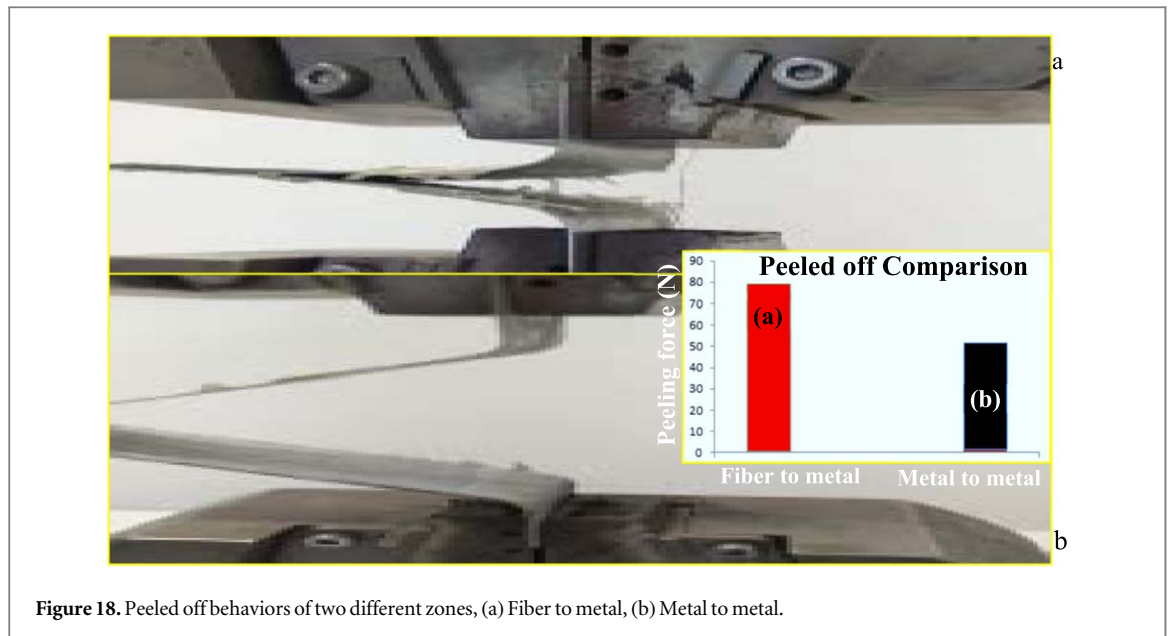
Figure 18. Peeled off behaviors of two different zones, (a) Fiber to metal, (b) Metal to metal.

Table 3. All types of composite performance with different response's on the basis of qualitative analysis.

Qualitative analysis of composite performance

Test	Responses'	3/2 Composite plies			4/2 Composite plies		
		0°	45°	90°	0°	45°	90°
Density (g/cm^3)	Thickness (mm)	low	low	low	Moderate	Moderate	High
	Mass (g)	low	moderate	low	Moderate	High	High
Axial tensile strength (N/m^2)	Stress (N)	High	low	Moderate	Moderate	Moderate	Moderate
	Strain (%)	High	Moderate	Moderate	Moderate	High	High
Flexural strength (MPa)	Flexural stress (N)	Moderate	low	low	Moderate	Moderate	low
	Flexural displacement (m^2)	High	High	Moderate	Moderate	low	low
Peeling Strength (N/m^2)	Load (N)	Moderate to high			Low to moderate		
	displacement (m^2)	Low to moder			Low to moderate		

3.2.3. Interlaminar peeling test

The span-to-depth ratio has dominated the failure mode of the specimens in interlaminar peeling tests. The adhesive layers undoubtedly significantly impact the interlaminar properties of FMLs. However, failure behaviors differ between FMLs with different adhesive bonding (see figure 17(b)). When the adhesive bonding with fiber to metal and metal to metal substrates is changed, the valid failure behavior mode is obtained.

Failure behavior is main fact of splitting the different layers. The two different combinations of layers are mentioned in figure 17(b). The layers have existence with fiber to metal inhaul the value around of force per mm is around 80. This layer has 3/2 composite plies. As shown in figure 17(b) the graph line produces very un-equity during the peeling off in the effective region. However, layers had distributed the force in different regions.

Hence, the test has the other combination of layers which were having the combination of metal to metal layers. These layers had revealed that the maximum force of peeling which can bear metal to metal layer combination with adhesive is around 50 N mm^{-1}. However, layers had uniformity in the force during the observation as compared to fiber to metal layers. Both combinations have shown less difference as an account of displacement (mm).

Generally, the theory of Metal Volume Fraction (MVF) [47], having been acknowledged to expect the properties of FMLs, emphasizes that the individual components control the overall performance of the FMLs. However, according to our research study, ignoring interlaminar failure is a necessary condition for MVF theory to work. In other words, the theory can only be used if the FMLs have the required interfacial bonding strength. The increased adhesive quantity causes the laminates to thicken, resulting in a lower volume fraction of glass fibers, which is damaging to the FMLs' strength. Even during the initial period, the peeling strength improves which confirming the positive function of the interfacial interaction as shown in figures 18(a), (b).

Figure 18 has revealed spoliation of layers and shows the interfacial bonding of adhesive with layers. The fiber to metal bonding zone figure 18(a) has separated very much sticky during the peeling test. The peak value of fiber to metal achieved during the test was 78 N mm^{-1}. normally; fiber and metal are good responders with adhesive. Another side in figure 18(b) metal to metal bonding is very loose and loses the adhesive bonding very easily during the peeling test and the peak value was 48 N mm^{-1}. Table. 3 has despite the performance of all composite concerning qualitative analysis and their responses.

4. Conclusion

Based on experimental results, the adhesive layers have improved the FMLs' interlaminar properties significantly. However, the mechanical properties of FMLs were dominated by two opposing factors. The density, tensile, and flexural properties were greatly improved during the initial period of around 5 to 10% instead, based on the range of the investigated adhesive and combined zone, with different parameters having been studied. The conclusions have revealed below facts:

(1) The types of composite have revealed the performance on different physical properties; most of the analysis 3/2 composite show better and enhanced physical analysis values.

(2) The most variant factor was the fiber orientation; mostly 0° orientation shows the better resistance to deformation in both the composite plies.

(3) The role of fiber volume fraction % during the fabrication of the composite and the impact of stress with different amounts of material.

(4) Meanwhile, peeling tests have revealed the interfacing bonding between fiber, metal, and adhesive as compared to metal and metal bonding.

(5) The concluded statement has fewer plies composite showing better structure deformation than the high number of plies.

Data availability statement

CRediT authorship contribution statement

Syed Qutaba: Conceptualization, Methodology, Literature review, Fabrication, Analysis and Writing. Mebrahitom Asmelash: Collecting the data, Writing, Citation, Administration and Drafting. Azmir Azhari: Conceptualization, Methodology, Design layout, Review, Funding acquisition and Supervision.

Declaration of competing interest

Authors declare, have no known competing financial interests.

ORCID iDs

Syed Qutaba https://orcid.org/0000-0003-2328-0466

References

[1] Xia Y, Wang Y, Zhou Y and Jeelani S 2007 Effect of strain rate on tensile behavior of carbon fiber reinforced aluminum laminates *Mater. Lett.* **61** 213–5
[2] Salve A, Kulkarni R and Mache A 2016 A review: fiber metal laminates (FML's)-manufacturing, test methods and numerical modeling *Int. J. Eng. Technol. Sci.* **3** 71–84

[3] Russig C, Bambach M, Hirt G and Holtmann N 2014 Shot peen forming of fiber metal laminates on the example of GLARE® *Int. J. Mater. Form.* **7** 425–38

[4] Lee B E, Park E T, Kim J, Kang B S and Song W J 2014 Analytical evaluation on uniaxial tensile deformation behavior of fiber metal laminate based on SRPP and its experimental confirmation *Compos. Part B Eng.* **67** 154–9

[5] Asundi A 2017 CAF metal laminates: an advanced material for future, 1997*aircraft. JMPT* **63** 384e94 aircraft. JMPT

[6] Fu Y, Zhong J and Chen Y 2014 Thermal postbuckling analysis of fiber–metal laminated plates including interfacial damage *Compos. Part B Eng.* **56** 358–64

[7] Sathishkumar T P, Satheeshkumar S and Naveen J 2014 Glass fiber-reinforced polymer composites–a review *J. Reinf. Plast. Compos.* **33** 1258–75

[8] Bagci M 2017 Influence of fiber orientation on solid particle erosion of uni/multidirectional carbon fiber/glass fiber reinforced epoxy composites *Proc. Inst. Mech. Eng. Part J J. Eng. Tribol.* **231** 594–603

[9] Qutaba S, Asmelash M, Saptaji K and Azhari A 2022 A review on peening processes and its effect on surfaces *Int. J. Adv. Manuf. Technol.* **120** 4233–70

[10] Rajan B S and Balaji M A S 2019 AB MAN. Effect of silane surface treatment on the physico-mechanical properties of shell powder reinforced epoxy modified phenolic friction composite *Mater. Res. Express* **6** 65315

[11] Sahin B and Kaya T 2019 Electrochemical amperometric biosensor applications of nanostructured metal oxides: A review *Mater. Res. Express* **6** 42003

[12] Pethrick R A 2012 9 - Composite to metal bonding in aerospace and other applications *Chaturvedi MCBTW and J of AM, editor. Woodhead Publishing Series in Welding and Other Joining Technologies [Internet]*. (India: Matthew Deans) 288–319

[13] Nissan A B and Findley K O 2014 12.16 - Microstructures and Mechanical Performance of Induction-Hardened Medium-Carbon Steels ed S Hashmi *et al Yilbas BBTCMP* (Oxford: Elsevier) 581–604

[14] Sugiman S, Crocombe A D and Katnam K B Investigating the static response of hybrid fibre–metal laminate doublers loaded in tension *Compos. Part B Eng.* 2011 **42** 1867–84

[15] Quan D, Wang G, Zhao G and Alderliesten R 2022 On the fracture behaviour of aerospace-grade Polyether-ether-ketone composite-to-aluminium adhesive joints *Compos Commun [Internet]*. **30** 101098

[16] Han J *et al* 2020 Effect of mechanical surface treatment on the bonding mechanism and properties of cold-rolled Cu/Al clad plate *Chinese J. Mech. Eng.* **33** 1–13

[17] Cortes P and Cantwell W J 2005 The fracture properties of a fibre–metal laminate based on magnesium alloy *Compos. Part B Eng.* **37** 163–70

[18] Frizzell R M, McCarthy C T and McCarthy M A 2008 An experimental investigation into the progression of damage in pin-loaded fibre metal laminates *Compos. Part B Eng.* **39** 907–25

[19] Zhan H, Lin J H, Shi H L and Wang J N 2021 Construction of carbon nanotubes/bismaleimide composite films with superior tensile strength and toughness *Compos. Sci. Technol.* **214** 108975

[20] Zaman I and Awang M K 2009 Influence of fiber volume fraction on the tensile properties and dynamic characteristics of coconut fiber reinforced composite *J. Sci. Technol.* **1** 1

[21] Yu G *et al* 2022 Transverse tensile mechanical experimental method and behavior of ceramic matrix mini-composites *Compos. Struct.* **297** 115923

[22] Feng Z *et al* 2019 Modification of surface treatment on the strength of 30CrMnSiA steel adhesively bonded joints *Mater. Res. Express* **6** 116521

[23] Eddahbi M, Thomson C B, Carreño F and Ruano O A 2000 Grain structure and microtexture after high temperature deformation of an Al–Li (8090) alloy *Mater. Sci. Eng. A* **284** 292–300

[24] Primee S Y and Juijerm P 2019 Modified mechanical surface treatment for optimized fatigue performance of martensitic stainless steel *Met. Mater. Int.* **27** 946–52

[25] Xue J, Wang W X, Takao Y and Matsubara T 2011 Reduction of thermal residual stress in carbon fiber aluminum laminates using a thermal expansion clamp *Compos. Part A Appl. Sci. Manuf.* **42** 986–92

[26] Kanchanomai C, Rattananon S and Soni M 2005 Effects of loading rate on fracture behavior and mechanism of thermoset epoxy resin *Polym. Test* **24** 886–92

[27] Gohel G, Bhudolia S K, Kantipudi J, Leong K F and Barsotti R J Jr 2020 Ultrasonic welding of novel Carbon/Elium® with carbon/epoxy composites *Compos. Commun.* **22** 100463

[28] Bagci M and Imrek H 2013 Application of Taguchi method on optimization of testing parameters for erosion of glass fiber reinforced epoxy composite materials *Mater. Des.* **46** 706–12

[29] Ravindra A, Dwarakadasa E S, Srivatsan T S, Ramanath C and Iyengar K V V 1993 Electron-beam weld microstructures and properties of aluminium-lithium alloy 8090 *J. Mater. Sci.* **28** 3173–82

[30] Wanhill R J H 1994 Status and prospects for aluminium-lithium alloys in aircraft structures *Int. J. Fatigue* **16** 3–20

[31] Han B, Tao W, Chen Y and Li H 2017 Double-sided laser beam welded T-joints for aluminum-lithium alloy aircraft fuselage panels: Effects of filler elements on microstructure and mechanical properties *Opt. Laser Technol.* **93** 99–108

[32] Li H *et al* 2019 The shot peen forming of fiber metal laminates based on the aluminum-lithium alloy: deformation characteristics *Compos. Part B Eng.* **158** 279–85

[33] Li H *et al* 2015 Reinforcement effects of aluminum–lithium alloy on the mechanical properties of novel fiber metal laminate *Compos. Part B Eng.* **82** 72–7

[34] Grinspan A S and Gnanamoorthy R 2006 A novel surface modification technique for the introduction of compressive residual stress and preliminary studies on Al alloy *Surf. Coatings Technol.* **201** 1768–75

[35] Tong Z *et al* 2019 Improvement in cavitation erosion resistance of AA5083 aluminium alloy by laser shock processing *Surf. Coatings Technol.* **377** 124799

[36] Akkurt A 2015 The effect of cutting process on surface microstructure and hardness of pure and Al 6061 aluminium alloy. *Eng Sci Technol an Int. J.* **18** 303–8

[37] Papenberg N P, Gneiger S, Weißensteiner I, Uggowitzer P J and Pogatscher S 2020 Mg-alloys for forging applications—a review *Materials* **13** 985

[38] Vo T P, Guan Z W, Cantwell W J and Schleyer G K 2013 Modelling of the low-impulse blast behaviour of fibre–metal laminates based on different aluminium alloys *Compos. Part B Eng.* **44** 141–51

[39] Partridge P G 1990 Oxidation of aluminium-lithium alloys in the solid and liquid states *Int. Mater. Rev.* **35** 37–58

[40] Ding H and Shin Y C 2012 Dislocation density-based modeling of subsurface grain refinement with laser-induced shock compression *Comput. Mater. Sci.* **53** 79–88

[41] Bo W, Chen X H, Pan F S, Mao J J and Yong F 2015 Effects of cold rolling and heat treatment on microstructure and mechanical properties of AA 5052 aluminum alloy *Trans. Nonferrous Met. Soc. China* **25** 2481–9

[42] Mansourinejad M and Mirzakhani B 2012 Influence of sequence of cold working and aging treatment on mechanical behaviour of 6061 aluminum alloy *Trans. Nonferrous Met. Soc. China* **22** 2072–9

[43] Pu Y, Hu J, Yao T, Li L, Zhao J and Guo Y 2021 Influence of anodization parameters on film thickness and volume expansion of thick- and large-sized anodic aluminum oxide film *J Mater. Sci. Mater. Electron.* **32** 13708–18

[44] Ravi S, Iyengar N G R, Kishore N N and Shukla A 2000 Influence of fiber volume fraction on dynamic damage in woven glass fabric composites: an experimental study *Adv. Compos. Mater.* **9** 319–34

[45] Luo J, Vargheese K D, Tandia A, Hu G and Mauro J C 2016 Crack nucleation criterion and its application to impact indentation in glasses *Sci. Rep.* **6** 1–10

[46] Li H *et al* 2019 The shot peen forming of fiber metal laminates based on the aluminum-lithium alloy: Deformation characteristics *Compos. Part B Eng.* **158** 279–85

[47] Wu H F, Wu L L, Slagter W J and Verolme J L 1994 Use of rule of mixtures and metal volume fraction for mechanical property predictions of fibre-reinforced aluminium laminates *J Mater. Sci.* **29** 4583–91